

Time-Domain CPC Decomposition: Answers to Comments on “Physical Interpretation of the Reactive Power in Terms of CPC Power Theory Revisited”

Dimitri Jeltsema and Jacob van der Woude

Summary: This note addresses some issues raised in [4] and refines some assertions made in our previous work on the time-domain Currents' Physical Components (CPC) decomposition in [10].

Key Words:
power theory,
reactive power,
current's physical
components

1. TIME-DOMAIN CPC DECOMPOSITION

For ease of reference, we start by recalling our time-domain CPC decomposition of [10]. Consider a single-input single-output (SISO) linear and time-invariant (LTI) system of the form

$$\dot{x}(t) = \mathcal{A}x(t) + \mathcal{B}v(t), \quad (1) \quad \text{and}$$

$$y(t) = \mathcal{C}x(t) + \mathcal{D}v(t),$$

where $x(t)$ denotes the state of the system, and the input $v(t)$ and the output $y(t)$ form a so-called power conjugated input-output pair, i.e., their product equals (instantaneous) power. If the input represents a voltage, then the output necessarily represent a current, and vice-versa. The matrices \mathcal{A} , \mathcal{B} , \mathcal{C} , and \mathcal{D} are constant matrices of appropriate dimensions reflecting the network structure of the load. Under the assumption that the system is stable, and some integrable periodic input $v(t)$, the stationary periodic solution of the system (1) is given by

$$y^*(t) = \int_{-\infty}^{\infty} h(s)v(t-s)ds = \int_0^{\infty} h(s)v(t-s)ds \quad (2)$$

where $h(t) := \mathcal{C}e^{\mathcal{A}t}\mathcal{B} + \mathcal{D}\delta(t)$ for $t \geq 0$ and $h(t) = 0$ for $t < 0$. Here $\delta(t)$ represents the Dirac distribution and the function $h(t)$ is called the impulse response. The key observation now is that the impulse response can be decomposed into an even and an odd part

$$\begin{aligned} h_e(t) &:= \frac{h(t) + h(-t)}{2}, \\ h_o(t) &:= \frac{h(t) - h(-t)}{2}, \end{aligned} \quad (3)$$

satisfying $h(t) = h_e(t) + h_o(t)$. Hence, we decompose $y^*(t)$ into

$$y_{||}^*(t) := \int_{-\infty}^{\infty} h_e(s)v(t-s)ds \quad (4)$$

$$= \int_0^{\infty} \frac{h(s)v(t-s)}{2}ds + \int_{-\infty}^0 \frac{h(-s)v(t-s)}{2}ds,$$

$$y_{\perp}^*(t) := \int_{-\infty}^{\infty} h_o(s)v(t-s)ds \quad (5)$$

$$= \int_0^{\infty} \frac{h(s)v(t-s)}{2}ds - \int_{-\infty}^0 \frac{h(-s)v(t-s)}{2}ds.$$

Hence, we claim in [10] that, for the case that $v(t) = u(t)$ is representing the source voltage and $y(t) = i(t)$ the associated load current, the active, scattered, and reactive current are given by

$$i_a(t) \equiv y_a^*(t) = G_e v(t),$$

$$i_s(t) \equiv y_s^*(t) = y_{||}^*(t) - G_e v(t) = y_{||}^*(t) - y_a^*(t), \quad (6)$$

$$i_r(t) \equiv y_r^*(t) = y_{\perp}^*(t),$$

respectively, where

$$G_e := \frac{\frac{1}{T} \int_0^T v(t)y^*(t)dt}{\frac{1}{T} \int_0^T v^2(t)dt} \quad (7)$$

represents the equivalent load conductance [3].

2. THE KRAMERS-KRONIG RELATIONS

Instrumental in our time-domain CPC decomposition (6) are the Kramers-Kronig relations. In essence, these relations provide a one-to-one correspondence between the even part and the odd part of the impulse response function in the time-domain and the real part and the imaginary part of its associated transfer function in the frequency-domain, respectively. In the original CPC decomposition [3], the role of the transfer function is played by the complex load admittance

$$Y(j\omega) = G(\omega) + jB(\omega), \quad (8)$$

which is a Hermitian function satisfying $Y(-j\omega) = \overline{Y(j\omega)}$ where (\cdot) represents the complex conjugation operator. Causality of the impulse response function, i.e., $h(t) = 0$ for $t < 0$, is crucial for the existence of the Kramers-Kronig relations. Hence, we claimed the relations

$$h_e(t) \leftrightarrow G(\omega), \quad h_o(t) \leftrightarrow B(\omega), \quad (9)$$

and referred to Figure 3 of [10] for a pictorial representation of this one-to-one correspondence between the time-domain and the frequency-domain. In [4] the authors state:

“Such a proof is needed especially because the illustration of the Kramers-Kronig relationship in Fig. 3 (ed. of [10]) is erroneous.”

Indeed, the graphs in Figure 3 of [10] representing the frequency-domain are mixed-up (the real and imaginary parts are reversed) and hence caused doubt of the correctness of (9), and thus of (6), by the authors of [4]. A correct pictorial representation of the Kramers-Kronig relations is depicted in Figure 1. For a constructive mathematical proof, we refer to the book [6].

3. TOWARDS AN INSTANTANEOUS CPC DECOMPOSITION

In [4], the authors ask the legitimate questions:

“The results of Section 1 (ed. Section 4 in [10]) are promising, but some conditions require clarification. ... First, over what interval of time does the input voltage $u(t)$ have to be integrable: over a period T or over infinity? How are the scalar product and rms value defined? The period of quantities involved in the energy transfer does not occur in Section 1 (ed. Section 4 in [10]); thus, are the results obtained valid for non-periodic quantities? Are these quantities of finite energy or finite power? If the decomposition, as presented in Section 1 (ed. Section 4 in [10]), is valid for quantities of finite energy, then this decomposition would be a time-domain equivalent of the CPC-based power theory of LTI systems with non-periodic quantities, developed in the frequency-domain, as presented in Ref. [1].”

In general, the time evolution of $y(t)$ in the interval $[0, t]$ can be computed from

$$y(t) = Ce^{At}x(0) + \int_0^t h(s)v(t-s)ds, \quad (10)$$

where $x(0)$ denote the initial conditions at $t=0$. The latter expression holds for any (locally) integrable input $v(t)$, periodic or non-periodic. From a system-theoretic point of view one is usually interested in ‘bounded-input and bounded-output’ (BIBO) stability. A system is BIBO stable if the output response to an input with finite amplitude has finite amplitude, i.e., if $\|v\|_\infty < \infty$ implies $\|y\|_\infty < \infty$. A necessary and sufficient condition is that the ‘action’ of the impulse response is finite, i.e.,

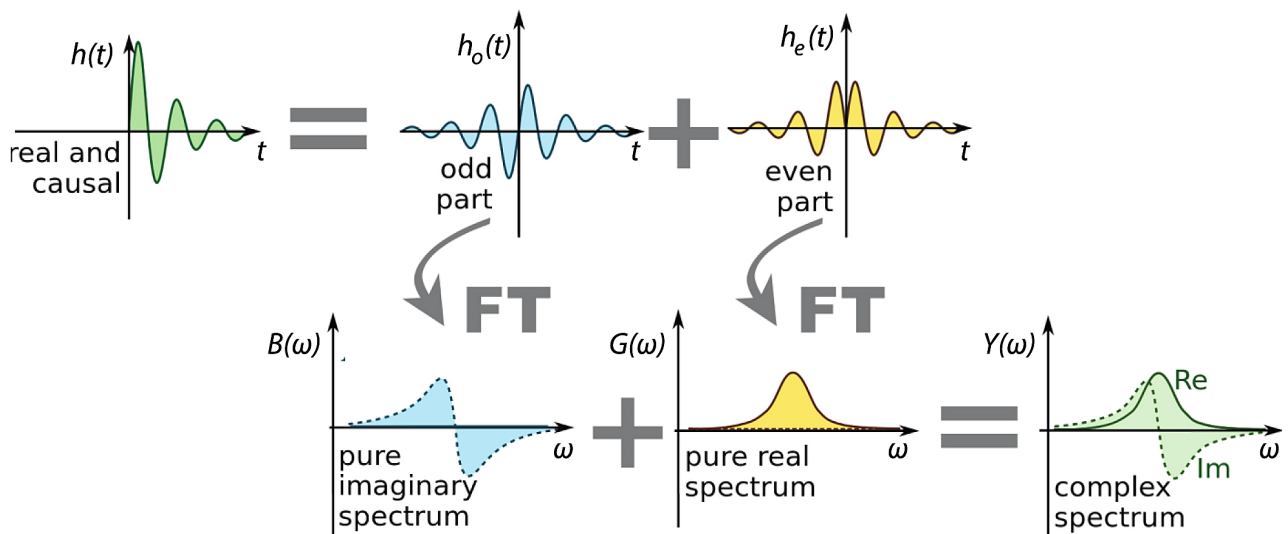


Fig. 1. The (correct) Kramers-Kronig relations for the case that $v(t) = u(t)$ represents the voltage source and $y(t) = i(t)$ represents the load current.

$$\|h\|_1 = \int_0^\infty |h(t)| dt < \infty \quad (11)$$

so that $\|y\|_\infty \leq \|h\|_1 \|v\|_\infty$. This condition is satisfied when the load network is asymptotically stable, i.e., when all the eigenvalues of the matrix \mathcal{A} are located in the open left half of the complex plane. However, in the exposition of Section 1 it is assumed that $v(t)$ is periodic and therefore is of the same form as in [3] (see also (12) in Section 4) in order to establish a one-to-one correspondence with the original CPC method—though with the exception that the number of harmonics may be infinite [9]. Moreover, it should be stressed that the periodicity assumption is necessary for (2) to make sense in a CPC context in order to guarantee orthogonality of the current decomposition.

The idea behind (2) is best explained using a sinusoidal input, say of the form $v(t) = \cos(\omega t)$. Under the assumption that the initial conditions are zero, the output $y(t)$ then reads

$$\begin{aligned} y(t) &= \int_0^t h(s) \cos(\omega(t-s)) ds \\ &= \int_0^\infty h(s) \cos(\omega(t-s)) ds - \int_t^\infty h(s) \cos(\omega(t-s)) ds. \end{aligned}$$

Now, the first right-hand term represents the sinusoidal steady-state response and the second right-hand term decays with time (i.e., the transient) if the system is stable. Under the condition that the system is stable, the sinusoidal steady-state response can be written as

$$\begin{aligned} y^*(t) &= \int_0^\infty \frac{h(s)}{2} \left(e^{j\omega(t-s)} + e^{-j\omega(t-s)} \right) ds \\ &= \frac{e^{j\omega t}}{2} \int_0^\infty h(s) e^{-j\omega s} ds + \frac{e^{-j\omega t}}{2} \int_0^\infty h(s) e^{j\omega s} ds. \end{aligned}$$

Note that the integrals represent the Fourier transforms of $h(t)$ and $h(-t)$, respectively. Hence, we can write

$$y^*(t) = \operatorname{Re}\{H(j\omega)\} \cos(\omega t) - \operatorname{Im}\{H(j\omega)\} \sin(\omega t).$$

Depending on the choice of the input and the output, $H(j\omega)$ can either represent the load admittance $Y(j\omega)$ or the load impedance $Z(j\omega) = Y^{-1}(j\omega)$. This means that the decomposition of Section 1 also allows a dual CPC decomposition, i.e., a CPC decomposition of a load that is driven by a current source. As for LTI systems the superposition theorem holds, the input can be any composition of sinusoidal functions.

Since the input $v(t)$ is assumed to be periodic with period T , the associated stationary output $y^*(t)$ is periodic with period T as well and the inner product and the rms values are defined as usual: the active power associated to (6) is defined as

$$P_a = \langle v, y^* \rangle = \frac{1}{T} \int_0^T v(t) y^*(t) dt = \|v\| \|y^*\|,$$

whereas the scattered power and the reactive power are

$$D_s = \|v\| \|y_s^*\| \text{ and } Q_r = \|v\| \|y_r^*\|,$$

respectively, where

$$\|\cdot\| = \sqrt{\frac{1}{T} \int_0^T (\cdot)^2 dt}$$

denotes the rms value.

In principle, starting from (10), an instantaneous and non-periodic version of (6) can be generated by considering, instead of (2), the general solution (10) and integrate (4) and (5) over the interval $[-t, t]$. Boundedness of the respective outputs to a bounded input is again given by (11) and can be associated to any (Lebesgue) norm, if it exists. Indeed, let v be locally integrable and defined on a subset \mathbb{D}^+ of the non-negative real axis. If $\|v\|_p < \infty$ and $\|h\|_1 < \infty$, then $\|y\|_p \leq \|h\|_1 \|v\|_p$, with

$$\|\cdot\|_p = \left(\int_{\mathbb{D}^+} |\cdot|^p dt \right)^{1/p}$$

for $1 \leq p < \infty$, and $\|\cdot\|_\infty = \sup_{t \in \mathbb{D}^+} |\cdot|$ for $p = \infty$. Note that $\|\cdot\|_2^2$ (the square of the 2-norm) defines the ‘energy’ of the signal. Hence, if $\|v\|_2^2$ exists, then $\|y\|_2^2 \leq \|h\|_1^2 \|v\|_2^2$ is well defined and of finite ‘energy’.

In a non-periodic setting, the inner product should be replaced by a moving average, whereas the rms values should be replaced by appropriate non-periodic equivalents. If the energy of the input and output is not finite, as is the case for quasi-periodic voltages and currents, such as inter- and subharmonics, the inner product is replaced by

$$\langle v, y \rangle = \lim_{T \rightarrow \infty} \frac{1}{T} \int_0^T v(t) y(t) dt,$$

representing the (average) ‘power’ with corresponding rms norm $\|\cdot\| = \sqrt{\langle \cdot, \cdot \rangle}$. We are currently studying the possibility of an instantaneous and non-periodic CPC decomposition. The results and their comparison to the work in [1] will be published elsewhere.

4. PHYSICAL PHENOMENA IN THE LOAD

Furthermore, in [4], a key issue is brought forward:

“Assuming that indeed current $y_\perp^*(t)$ is the reactive current, then how is this current associated with a physical phenomenon in the load, without going outside of the time-domain concept, meaning not using terms from the frequency-domain, such as ‘the phase-shift’, ‘harmonics’, and ‘susceptance’? All that was told above about the reactive current applies also to the scattered current.”

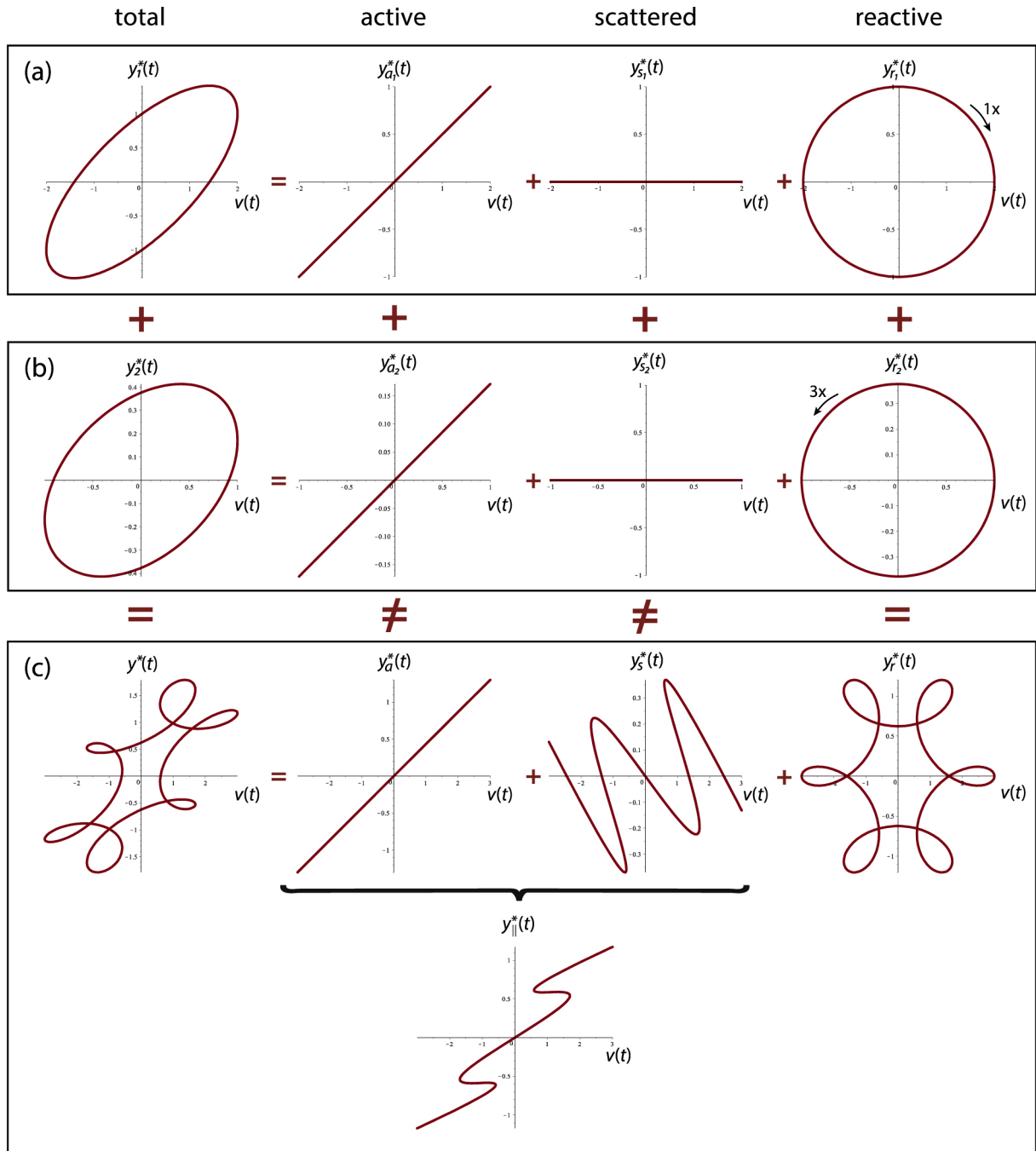


Fig. 2. Lissajous plots illustrating the time-domain character of active, scattered, and reactive current for (a) $v_1(t)=2\sin(t)$; (b) $v_1(t)=\sin(5t)$; and (c) $v(t)=2\sin(t)+\sin(5t)$. Obviously, only the Lissajous plots on the left can be measured in reality.

The original CPC decomposition [3] is founded on the Fourier series of the input signal (the DC component V_0 is omitted for ease of presentation)

$$v(t) = \sqrt{2} \operatorname{Re} \left\{ \sum_{n \in N} V_n e^{jn\omega t} \right\} = \sum_{n \in N} v_n(t), \quad (12)$$

where N is the set of harmonics present in the signal and $\omega=2\pi/T$ is the fundamental frequency. The advantage of such representation is that the harmonic content of the signal provides an orthogonal basis on which the CPC current harmonics associated with the active, scattered, and

reactive phenomena are projected. Orthogonality is essential to perform an apparent power decomposition. Expressing a given periodic input signal and its output response in terms of a Fourier series enables one to define the phase-shift between two input-output harmonics with the same frequency. Nevertheless, the Fourier series representation of a periodic time-domain signal is artificial.

In general, it will be hard (if not impossible) to define the ‘phase-shift’ from just two periodic signals without going into their harmonic content. It will also be impossible to provide an interpretation of the phenomena supporting the scattered and reactive current components using the time-domain framework presented in Section 1 on the same footing as

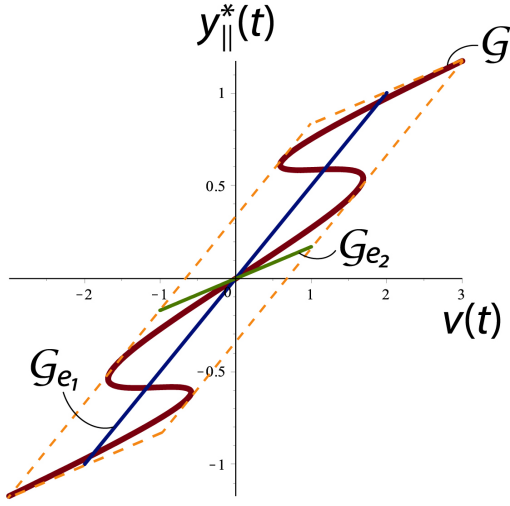


Fig. 3. Lissajous plot exhibiting the nonlinear-like behavior of $y_{\parallel}^*(t)$ versus $v(t) = v_1(t) + v_2(t)$.

in [3], but without referring to (12). Nevertheless, as any property defined in the frequency-domain has its time-domain counterpart, there should exist time-domain equivalents to the frequency-domain notions used in [3].

Real-world phenomena are observed in the time-domain and physical systems are causal, which is reflected by the condition $h(t) = 0$ for $t < 0$. It is clear from Figure 1 that the even-odd decomposition of $h(t)$ leads to impulse responses associated to non-causal systems as $h_e(t)$, $h_o(t) \neq 0$ for $t < 0$. Any current or voltage derived from these impulse responses is inherently non-physical in nature. Consequently, the explanation that the presence of the reactive current in nonsinusoidal situations is due to a phase-shift between the individual harmonics and that the scattered current is due to a change of the load conductance with harmonic order is therefore artificial as such phenomena are (by itself) not collectively observable in the real-world. This does of course not mean that such interpretations are useless.

One way to avoid the notion of harmonics is to consider the concept of (cross-)correlation. However, such approach will have a mathematical character rather than that it provides physical insights. An oscilloscope, on the other hand, is a tool commonly used to visualize real-world signals in the time domain. For that, an appealing way to interpret the time-domain origin of the scattered and the reactive current, without referring to the harmonic content (12), is the use of Lissajous plots. Let us start with the scattered current.

4.1. Time-Domain Origins of the Scattered Current

Consider an LTI series RLC load network with $R = 1$ [Ω], $L = 1/2$ [H], and $C = 2/3$ [F]. The impulse response is given by

$$h(t) = 2e^{-t} \cos(t\sqrt{2})1(t) - \sqrt{2}e^{-t} \sin(t\sqrt{2})1(t), \quad (13)$$

where $1(t)$ denotes the Heaviside step function. As (13) is the result of applying a Dirac distribution as the input voltage, it is clear that that we can not obtain any information

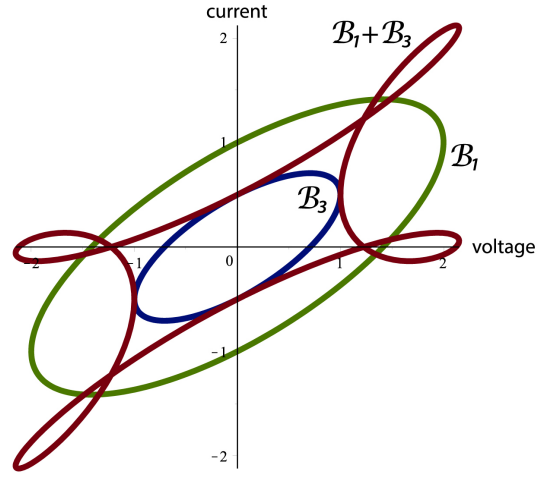


Fig. 4. Lissajous plot for $v_1(t) = 2\sin(t)$ (represented by B_1 in green), $v_3(t) = \sin(3t)$ (represented by B_3 in blue), and $v(t) = v_1(t) + v_3(t)$ (represented by $B = B_1 + B_3$ in red).

regarding the response to another input without considering (2). The behavior of the output of the system thus depends on the form of the applied input. Indeed, let us perform the following experiment. Suppose that subsequently the following sinusoidal voltages are applied: $v_1(t) = 2\sin(t)$ [V] and $v_2(t) = \sin(5t)$. The resulting load currents $y_1^*(t)$ and $y_2^*(t)$ are obtained from (2), which, according to (6), can be decomposed into the active components $y_{a_1}^*(t)$ and $y_{a_2}^*(t)$, scattered components $y_{s_1}^*(t)$ and $y_{s_2}^*(t)$, and reactive components $y_{r_1}^*(t)$ and $y_{r_2}^*(t)$. The corresponding Lissajous plots are shown in Figure 2 (a) and (b). Since the load is LTI, we have the property that if (v_1, y_1^*) and (v_2, y_2^*) are two input-output pairs, the linear combination $(\alpha v_1 + \beta v_2, \alpha y_1^* + \beta y_2^*)$ is also an input-output pair for arbitrary scalars α and β . However, although $v(t) = v_1(t) + v_2(t)$ implies $y(t) = y_1^*(t) + y_2^*(t)$, this does not hold for the active and scattered components as shown in Figure 2 (c), which suggests that, under nonsinusoidal conditions, the definitions of the active and scattered currents are nonlinear in nature.

From circuit-theory we know that any straight line through the origin in the current-voltage plane defines an LTI resistive or conductive constitutive relationship. Such resistor/conductor is passive if the constitutive relationship is confined to the first and the third quadrant. Hence, for the given load, the current-voltage relationship of the active current can be associated to an LTI conductance, which equals the equivalent load conductance G_e defined in (7). To clarify the time-domain origin of the scattered current $y_s^*(t)$ as the result of the combined voltage $v(t) = v_1(t) + v_2(t)$, let us consider the Lissajous plot of $y_{\parallel}^*(t) = y_{a_1}^*(t) - y_{a_2}^*(t)$ shown in Figure 3. Clearly, the current-voltage relationship does not exhibit a straight line through the origin and, hence, this characteristic suggests a nonlinear-like behavior. As shown in Figure 3, the curve is seen to be bounded by a parallelogram that is spanned by the principle axes defined by the lines $\mathcal{G}_{e_1}(v_1, y_{a_1}^*) = 0$ and $\mathcal{G}_{e_2}(v_1, y_{a_2}^*) = 0$ associated to the respective active components. The slopes of these lines are

G_{e_1} and G_{e_2} . Let d denote the differential operator, i.e., if a signal $z(t)$ is differentiable, $dz(t) = (dz(t))/dt$, then the slopes G_{e_1} and G_{e_2} can, instead of (7), also be defined by

$$G_{e_k} = \frac{dy_{a_k}^*}{dv_k} \quad (14)$$

for $k=1,2$. For the given choice of voltages $v_1(t)$ and $v_2(t)$, we have $G_{e_1} \neq G_{e_2}$, and thus the load current will contain a scattered component $y_s^*(t) \neq 0$. According to Figure 3, the instantaneous active power components $v_1(t)y_{a_1}^*(t)$ and $v_1(t)y_{a_2}^*(t)$ are 'scattered' within the parallelogram spanned by the lines $\mathcal{G}_{e_1}(v_1, y_{a_1}^*) = 0$ and $\mathcal{G}_{e_2}(v_1, y_{a_2}^*) = 0$.

However, if we apply a voltage $v_3(t) = \sin(3t)$, then we obtain $G_{e_3} = G_{e_1}$ and hence the scattered current associated to the input voltage $v_1(t) + v_3(t)$ will be zero as the lines $\mathcal{G}_{e_1}(v_1, y_{a_1}^*) = 0$ and $\mathcal{G}_{e_3}(v_3, y_{a_3}^*) = 0$ coincide. The original CPC power theory [3] explains this phenomenon based on the complex frequency-domain conductance $G(\omega)$. Indeed, taking the Fourier transform of the even part of (13) yields

$$\text{Re}\{H(j\omega)\} = \frac{4\omega^2}{\omega^4 - 2\omega^2 + 9} = G(\omega), \quad (15)$$

from which we observe that $G(1) = G(3)$ while $G(1) \neq G(5)$. Thus, according to [3], the scattered current arises due to changes in the load conductance with harmonic order.

In the time-domain, this phenomenon can be interpreted in terms of an incremental conductance. If $v(t)$ is differentiable (which is the case for any smooth periodic signal), then this incremental conductance is given by

$$G^* = \frac{dy_{||}^*}{dv}, \quad (16)$$

and represents the slope at each point on the curve $\mathcal{G}(v, y_{||}^*) = 0$. Thus, the scattered current can be considered as the current associated to an incremental conductance that is 'scattered' around the equivalent conductance, i.e., $G_s^* = G^* - G_e$ and represents the slope at each point on the curve $\mathcal{G}_s(v, y_s^*) = 0$. Note that due to the non-causal character of $h_e(t)$, the scattered conductance G_s^* can be either voltage-controlled or current-controlled, or both.

4.2. Time-Domain Origins of the Reactive Current

Consider again the LTI series network characterized by (13). In contrast to the active and scattered components, the reactive components does satisfy the linearity condition, i.e., for any input-output pairs $(v_1, y_{r_1}^*)$ and $(v_2, y_{r_2}^*)$, the linear combination $(\alpha v_1 + \beta v_2, \alpha y_{r_1}^* + \beta y_{r_2}^*)$ is also an input-output pair. Hence, for $v(t) = v_1(t) + v_2(t)$, we have $y_r^*(t) = y_{r_1}^*(t) + y_{r_2}^*(t)$. This means that the respective Lissajous plots shown in Figure 2 (a) and (b) at the right are additive, for which the combined result is shown at the right of Figure 2 (c). It is well-known that a phase-shift, or time-shift for that matter, between two sinusoidal signals with the same period can be detected from the associated Lissajous plot in the time-domain. Two sinusoidal signals that are

relatively shifted by a quarter period exhibit a circular shape that is centered around the origin as is observable from Figure 2 (a) and (b). The Lissajous plot of Figure 2 (c) exhibits an integral time-shift between $v(t)$ and $y_r^*(t)$.

Interestingly, it is observed from Figure 4 that for the input $v(t) = v_1(t) + v_3(t)$, the (absolute) time-shift between input-output pairs (v_1, y_1^*) and (v_3, y_3^*) is exactly the same. Recall that for this case $G(1) = G(3)$, implying a zero scattered current. In the frequency-domain, this suggests that the scattered current is also due to differences in (absolute) phase-shift between the individual input-output harmonics. This fact is not surprising as the load conductance and susceptance are related through the Kramers-Kronig relations. In the time-domain this one-to-one correspondence is simply expressed as $h_e(t) = \text{sgn}(t) h_o(t)$ and $h_o(t) = \text{sgn}(t) h_e(t)$, where $\text{sgn}(t)$ denotes the signum function. Hence, only the knowledge of either $h_e(t)$ or $h_o(t)$ is needed to determine the full system behavior.

Another (classical) interpretation of the existence of reactive current in time-invariant, (possibly nonlinear) systems is the imbalance between the magnetic and electric energies stored in the load inductors and capacitors, respectively. As energy and power are conserved when passing from the frequency-domain to the time-domain, and vice-versa, via Parseval's identity, such interpretation holds for both the frequency-domain and the time-domain. For details, see [5]. It should be stressed, however, that for time-varying systems reactive current can also exists in systems without any energy storage as illustrated in the following section.

5. THE TRIAC CIRCUIT RECONSIDERED

Concerning our power decomposition of the TRIAC circuit in [10], we fully agree with the remarks in [4]. Although our decomposition is mathematically correct, it has nothing to do with the CPC decomposition. In this section, we would like to take the opportunity to show that a proper application of the time-domain CPC decomposition provides the same results, though from a different angle, as in [2].

Consider the TRIAC circuit depicted in Figure 5 (a), with $u(t) = 220\sqrt{2} \sin(t)$ [V], a load resistance $R = 1\Omega$, and a switching angle $\alpha = 135^\circ$, the current-voltage relationship can be represented by the Lissajous plot shown in Figure 5 (b).

Although the approach outlined in Section 1 is (so far) established for linear time-invariant (LTI) systems, the extension to static time-dependent circuits, like the TRIAC circuit of Figure 5, can be taken into consideration as follows. Since there are no inductors and no capacitors in the circuit, the matrices \mathcal{A} , \mathcal{B} , \mathcal{C} and \mathcal{D} are all void. Hence, the system (1) changes to a static time-varying input-output system of the form

$$y(t) = y^*(t) = D(t) v(t), \quad (17)$$

where the input $v(t) = u(t)$ and the output $y(t) = i(t)$ represent the supply voltage and supply current, respectively, whereas the direct feed-through term $D(t)$ represents the load in the form of a time-varying linear conductor

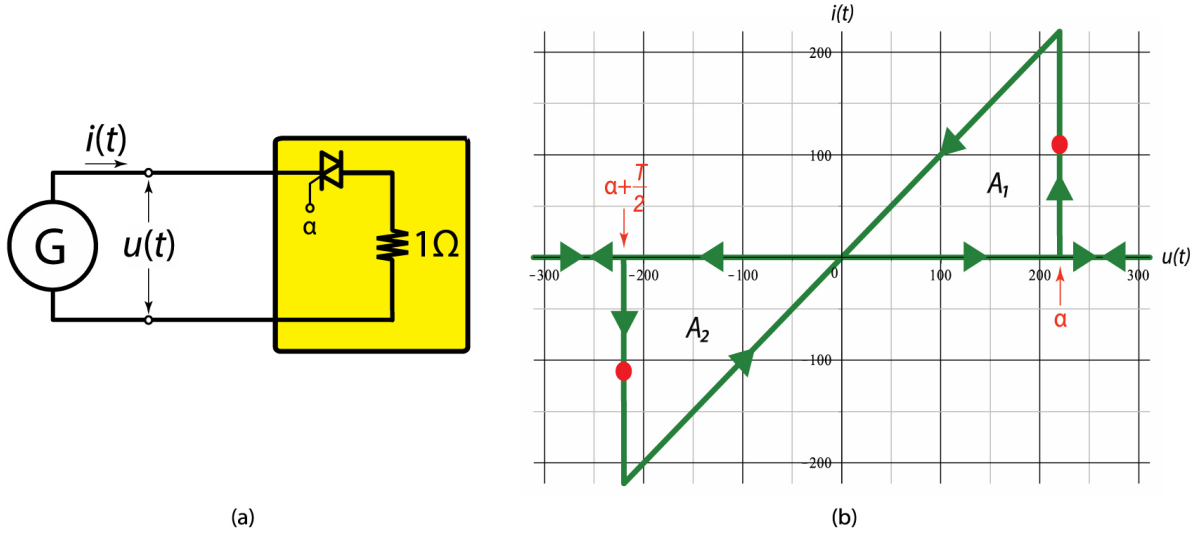


Fig. 5. Circuit with resistive load and TRIAC (a) and its corresponding Lissajous plot (b).

$$\mathcal{D}(t) = \begin{cases} 0 & \text{for } t \in \left[\frac{kT}{2}, \frac{kT}{2} + \alpha \right), k = 0, 1, 2, \dots, \\ 1 & \text{otherwise.} \end{cases}$$

As the circuit does not exhibit any dynamics, it is sufficient to consider only the first period: $k=0,1$. However, as the scattered and reactive currents in the CPC decomposition are defined relative to the supplied voltage it seems unavoidable to follow exactly the same steps as in [2] and decompose $y(t)$ in terms of a Fourier series and consider only the first terms, i.e., $y_1(t) = 40.317\sqrt{2} \sin(t - 60.28^\circ)$ [A]. Now, the conductance associated to the first harmonic is given by

$$\mathcal{D}_1(t) = \frac{y_1(t)}{v(t)} = 0.183 \frac{\sin(t - 60.28^\circ)}{\sin(t)} [\Omega^{-1}]$$

Next, we separate the even and odd parts of $\mathcal{D}_1(t)$ as follows:

$$y_{||}(t) = \frac{\mathcal{D}_1(t) + \mathcal{D}_1(-t)}{2} v(t) = 19.986\sqrt{2} \sin(t) [\text{A}],$$

$$y_{\perp}(t) = \frac{\mathcal{D}_1(t) - \mathcal{D}_1(-t)}{2} v(t) = -35.014\sqrt{2} \cos(t) [\text{A}],$$

which correspond to the active and reactive current, respectively. The harmonic components in the current that do not match the harmonic content of $v(t)$ are then given by $y_h(t) = v(t) - y_1(t)$ and the scattered current $y_s(t) = 0$. These currents precisely coincide with the ones obtained in [2]. It should be noted, however, that this example also shows the non-physical character of the CPC currents as the active and reactive currents are nonzero in the interval that the switch is not conducting, a phenomenon that will not be observed in the real-world.

For this particular example, the same result can also be obtained without using an explicit harmonic decomposition. Indeed, the active current can be computed directly in the time-domain using (7) as

$$y_a(t) = \frac{P_a}{\|v\|^2} v(t),$$

where $\|v\| = 220$ [V] and $P_a = \langle v, y \rangle = 4.396$ [kW]. The reactive current, on the other hand, can be obtained by considering an orthogonal projection of the total current on the time-derivative of the source voltage, i.e.,

$$y_r(t) = -\frac{\omega Q_I}{\|\dot{v}\|^2} \dot{v}(t),$$

where $\|\dot{v}\| = 220$ [V/s] and Q_I is defined as

$$Q_I = -\frac{1}{\omega T} \int_0^T \dot{v}(t) y(t) dt = 7.703 [\text{kVAr}].$$

The latter integral is known as the Iliovici reactive power [7,8] and represents a measure of the area $A_1 + A_2$ of Figure 5 (b). For more details, the reader is referred to [11].

6. CONCLUDING REMARKS

We have refined and corrected some assertions made in our previous work on the time-domain CPC decomposition in [10] and answers are provided to the various questions raised in [4]. It is shown that the time-domain origins of the scattered current can be related to the current- or voltage-dependent incremental character of the load conductance under nonsinusoidal conditions. Instrumental in the analysis is the use of Lissajous plots. Such plots also exhibit the time-domain character of the reactive current.

ACKNOWLEDGMENT

The first author would like to express his gratitude towards Prof. Hartman from the Gdynia Maritime University, Poland, for the fruitful discussions on the theory of power and pointing him to the existence of Iliovici's concept of reactive power. Both authors would like to thank Prof. Czarnecki and Mr. Haley from the Louisiana State University, USA, for their instructive remarks about and their encouragement of developing a true time-domain CPC decomposition.

REFERENCES

1. Czarnecki L.S. and A. Lasicz, "Active, reactive, and scattered currents in circuits with non-periodic voltage of a finite energy". IEEE Trans. Instr. Measur., Vol. IM-37, No. 3, pp. 398-402, Sept. 1988.
2. Czarnecki L.S. "Physical interpretation of reactive power in terms of the CPC power theory," Electrical Power Quality and Utilisation Journal, Vol. XIII, No. 1, pp. 89-95, 2007.
3. Czarnecki L.S. "Currents' Physical Components (CPC) concept: a fundamental power theory," Przegląd Elektrotechniczny, vol. R84, no. 6, pp. 28-37, 2008.
4. Czarnecki L.S. and P.L. Haley, "Comments on Physical Interpretation of the Reactive Power in Terms of CPC Power Theory Revisited", Electrical Power Quality and Utilisation Journal, Vol. XVI, No. 2, pp. 7-9, 2013.
5. García-Canseco Eloísa, Roberto Griño, Romeo Ortega, Miguel Salichis, and Aleksandar M. Stanković. Power-factor compensation of electrical circuits. IEEE Control Systems Magazine, 99:46-59, 2007.
6. Hall S.H. and H.L. Heck. Advanced Signal Integrity for High-Speed Digital Designs, John Wiley & Sons, Inc., 2009.
7. IEEE Standard 1459-2010, IEEE Standard Definitions for the Measurement of Electric Power Quantities Under Sinusoidal, Nonsinusoidal, Balanced, or Unbalanced Conditions, IEEE Power and Energy Society, 2010.
8. Illovici M. "Définition et Mesure de la Puissance et de L'Energie Réactives", Bull. Soc. Franc. Electr., n. 5, 931-954, 1925.
9. Jeltsema D. and J.W. van der Woude, "Currents' Physical Components (CPC) in the time-domain: single-phase systems," In proc. 13th European Control Conference, Strasbourg, France, 2014.
10. Jeltsema D. and J.W. van der Woude, "Physical Interpretation of the Reactive Power in Terms of CPC Power Theory Revisited, Electrical Power Quality and Utilisation Journal, Vol. XVI, No. 2, pp. 1-6, 2013.

11. Jeltsema D., J.W. van der Woude and M.T. Hartman, "A Novel Time-Domain Perspective of the CPC Power Theory: Single-Phase Systems," Submitted for publication. A preliminary version can be obtained from <http://arxiv.org/abs/1403.7842>.
12. Papoulis A., Fourier Integral and its Applications. New York: McGraw-Hill, 1962.



Dimitri Jeltsema

received the B.Eng. degree in electrical engineering from the Rotterdam University of Applied Sciences, The Netherlands, and the M.Sc. degree in systems and control engineering from the University of Hertfordshire, United Kingdom in 1996 and 2000, respectively. In May 2005 he received the Ph.D. degree with honors (cum laude) from Delft University of Technology, The Netherlands. Until 2007 he has been a post-doctoral researcher and lecturer at the Delft Center for Systems and Control. Currently he is an assistant professor at the Mathematical Physics Group of the Delft Institute of Applied Mathematics. His research includes systems and control theory of physical systems, power theory and power factor optimization, and nonlinear circuit theory.



Jacob van der Woude

received the M.S. degree in mathematics from the Rijksuniversiteit Groningen in 1981 and the Ph.D. degree from the Department of Mathematics and Computing Science, Eindhoven University of Technology, Eindhoven in 1987. In 1988 and 1989, he was a Research Fellow at the Center for Mathematics and Computer Science, Amsterdam. Since 1990, he is with the System Theory Group, Faculty of Electrical Engineering, Mathematics and Computer Science, Delft University of Technology, first as assistant professor and from 2000 onwards as associate professor. His current research interests include system and control theory, switching and power networks and applications of graph theory.